Hindawi
International Journal of Polymer Science
Volume 2023, Article ID 6685837, 12 pages
https://doi.org/10.1155/2023/6685837

Research Article

Virtual Fatigue Behaviour Analysis of Coir Fibre-Reinforced PVC Composites

Gopalan Venkatachalam,[1] Umapathy Jayanthi,[2] Arumugasamy Suja,[2] Senthil Gnanaaksaya,[2] Sampath Aravindh,[2] Pitchumani Shenbaga Velu,[2] Kulendran Balamurugan,[3] and Rajendiran Gopal[4]

[1]*Centre for Innovation and Product Development, Vellore Institute of Technology, Chennai 600127, Tamil Nadu, India*
[2]*School of Mechanical Engineering, Vellore Institute of Technology, Chennai 600127, Tamil Nadu, India*
[3]*Department of Mechanical Engineering, Government College of Engineering, Erode 638316, Tamil Nadu, India*
[4]*Automotive Engineering Program, Department of Mechanical and Industrial Engineering, Bahir Dar Institute of Technology, Bahir Dar, Ethiopia*

Correspondence should be addressed to Rajendiran Gopal; rajendiran.gopal@dec.edu.et

Received 3 June 2023; Revised 19 October 2023; Accepted 9 November 2023; Published 30 November 2023

Academic Editor: Yiqi Yang

PVC (polyvinyl chloride) is a tough polymer used in applications, including plumbing and construction materials. As natural fibre-reinforced composites have more advantages over conventional synthetic composites, this paper focuses on the fatigue analysis of PVC composite which is reinforced with coir fibre. The influences of three input parameters, namely, the size of the coir fibre, coir fibre content, and the chemicals that are used in the treatment of coir fibre on the fatigue life of the composite are examined. In the response surface model (RSM), Box-Behnken designs (BBD) are employed for the preparation/analysis/optimization of the samples. ANSYS software is used to perform the fatigue analysis of different samples containing various combinations of the parameters. To determine the effects of various input parameters on the fatigue behaviour of composites, ANOVA is employed to determine their optimal levels. Regression equations are established to determine the fatigue limit. When treated with triethoxy(ethyl)silane, coir with a concentration of 6 wt.% and a particle size of 75 μm exhibits a maximum fatigue limit of 2.819 MPa.

1. Introduction

PVC, often known as polyvinyl chloride, is a frequently used material because it is affordable, strong, and flexible. PVC is a hard thermoplastic used in various applications such as building materials, pipes, and plumbing [1]. PVC has the widest range of applications, and its use has increased more significantly than that of other polymers for a myriad of factors other than the affordability of the raw materials. This is because PVC is simple to manufacture and has a longer lifespan. PVC has much more strength, is more rigid than most other thermoplastics, and has exceptional chemical resistance to a wide spectrum of corrosive fluids [2].

Safety and environmental concerns should be considered when using PVC. An intriguing alternative is to combine PVC with natural fibres [1]. Natural fibres, which might be available in different forms such as particles, fibre bundles, or single fibres, can be utilized as either a filler or as a reinforcement in plastics. Instead of filling plastics, natural fibres can be utilized to reinforce them, giving them more strength and stiffness [3]. Natural fibre-reinforced composite materials are of tremendous interest because of their fine mechanical qualities, ecofriendliness, lightweight, exceptional life cycle, and biodegradability [4]. As a result, they are employed to replace more standard fibres like glass, carbon, and aramid [5]. Natural fibres, from sources including coir [6–8], oil palm [9], sisal [10, 11], bamboo [12], banana

Table 1: Various fibre content, size of fibre, and chemicals.

Variables	Parameters	Levels	-1	0	1
A	Fibre content	wt.% of material in composites	2	4	6
B	Size	Size of the fibre in μm	75	150	225
C	Chemical treatment	Chemicals used	1 (triethoxy(ethyl)silane)	2 (NaOH)	3 (KOH)

Table 2: BBD table of various combinations of the parameters.

Sample no.	Fibre content		Size		Chemical treatment	
	Coded	Actual	Coded	Actual	Coded	Actual
1	1	6	0	150	1	3
2	-1	2	0	150	-1	1
3	0	4	0	150	0	2
4	-1	2	-1	75	0	2
5	1	6	1	225	0	2
6	0	4	1	225	-1	1
7	0	4	1	225	1	3
8	0	4	0	150	0	2
9	0	4	-1	75	-1	1
10	0	4	-1	75	1	3
11	-1	2	0	150	1	3
12	1	6	0	150	-1	1
13	0	4	0	150	0	2
14	1	6	-1	75	0	2
15	-1	2	1	225	0	2

[13, 14], rice husk [15], jute [16, 17], and kenaf [18, 19], are shown to be effective reinforcement in polymeric matrices, lowering the density and expense of the resulting composites. Natural fibre composite mechanical properties are impacted by factors, namely, fibre selection, matrix selection, interface strength, fibre dispersion, and fibre orientation [20].

A few drawbacks of using natural fibres are low thermal stability (probable degradation between 200 and 250°C), owing to their hydrophilic nature and poor fibre adherence leading to fibre swelling and moisture content. In the micromechanical behaviour of composite, the fibre/matrix adherence plays a significant impact. Natural fibres absorb a lot of moisture and have poor adherence to the polymeric matrix [21].

Contrarily, the matrix is mostly made of polymers that naturally resist water such as polypropylene, polyvinyl chloride, and polylactic acid. Since natural fibres are hydrophilic and polymer matrixes are hydrophobic, there is weak interface bonding between the two. So, the natural fibre and polymer matrix do not adhere well to one another; therefore, the composites' mechanical performance decreases. Natural fibre surfaces can be easily altered to vary their hydrophilic character [22]. Numerous chemical processes are available to change the hydrophilic properties. Some of the treatments include alkaline treatment, acetylation of natural fibre, silane treatment, benzoylation treatment, permanganate treatment, maleated coupling agents, and isocyanate treatment [23, 24]. The alkaline treatment (5% NaOH), which helps to improve interactions between fibre and the matrix by attempting to remove hemicellulose, lignin, as well as waxy elements as an outcome of disrupting hydrogen bonding within fibre structure, is the most economical and effective chemical treatment, as per various chemical treatments, resulting in improved mechanical and thermal properties [25]. Venkatachalam et al. claimed that the optimum value of flexural stress was achieved by combining 45 fibre orientation, epoxy resin, and KMnO4 treatment of the fibre. These conclusions were based on taking into account many factors, including fabric orientation, the type of alkali treatment, the type of resin, and its impact on the fracture and flexural behaviours of sandwich panels reinforced with flax fibre. There is relatively little variation in flexural stress according to the alkali treatment method [26]. Based on Adeniyi et al.'s findings, alkalization with NaOH was the most widely used kind of treatment. In comparison to their treated counterparts, which have had the quantity of free hydroxyls reduced after treatment, untreated coir composites are more prone to excessive water absorption. The most researched polymer matrix for coir fibre-reinforced composites was polypropylene [27]. When considering various natural fibres for reinforcement, a lignocellulosic fibre called coir is one of the preferred choices cultivated from coconut trees in the tropics [28]. The majority of the planet's coir production, nearly 90%, is made in Sri Lanka and India. Contrary to certain other plant fibres, coir contains a lot of lignin (41-45%),

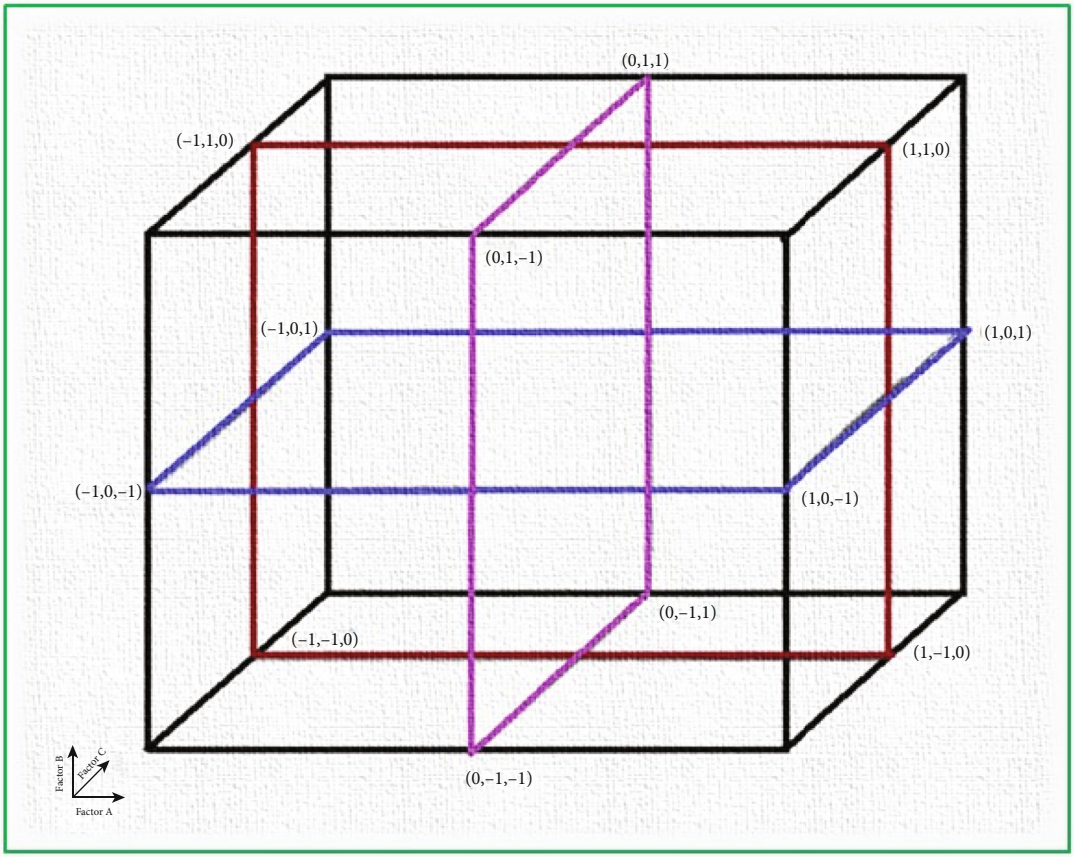

Figure 1: Box-Behnken design.

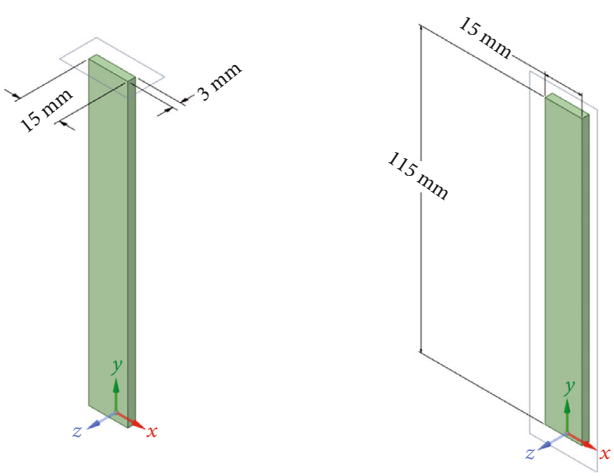

Figure 2: Geometry for the analysis.

making it a hard fibre renowned for endurance. When employed in humid environments, coir's high wet strength ratings are helpful [29]. In comparison to other natural fibres, coir fibres have some competitive advantages, such as low density, low cost, higher elongation at break, and a lower elastic modulus. Additionally, coir fibre typically has a density of 1.1 to 1.5 g/cm^3, a tensile strength of 105 to 593 MPa, and Young's modulus of 2 to 8 GPa [30, 31]. On the topic of the coir fibre made used in any composites, the percentage of the said fibre and the size of the fibre play a vital role in deciding the properties of the composite. According to the tensile test results conducted by Venkatachalam et al., epoxy combined with 10 mm jute fibre at 3% volume provides the maximum modulus of elasticity, yield stress, and modulus of resilience. They found that Young's modulus falls along with the percentage of jute. In comparison to epoxy/jute fibre specimens, coir fibre with a 1 mm length and 2% volume is a strong competitor [32]. When considering the overall size of the fibres present in the composite, Sadeq et al. have results based on the experiments conducted, where the size of the coir fibre reinforced in epoxy ranges from 250 μm to 950 μm, for which the flexural strength and impact strength are established to vary concerning the size of the coir. The flexural strength increases with the increasing range of the fibre size, and vice versa for the impact strength [33].

The mechanical properties of the composite samples, which were made with varying fibre contents ranging from 10 to 30% by weight, were also examined. When reinforced with 20% fibre loading by weight, polystyrene composites reinforced with raw as well as MMA-grafted agave fibres showed maximum mechanical strength [34]. However, when fibre loading increases, Young's modulus of polymer composites reinforced with natural fibres also rises. With increasing fibre loading, the tensile strength and modulus of elasticity of composites which have been reinforced with bleached hemp fibres have significantly increased, according

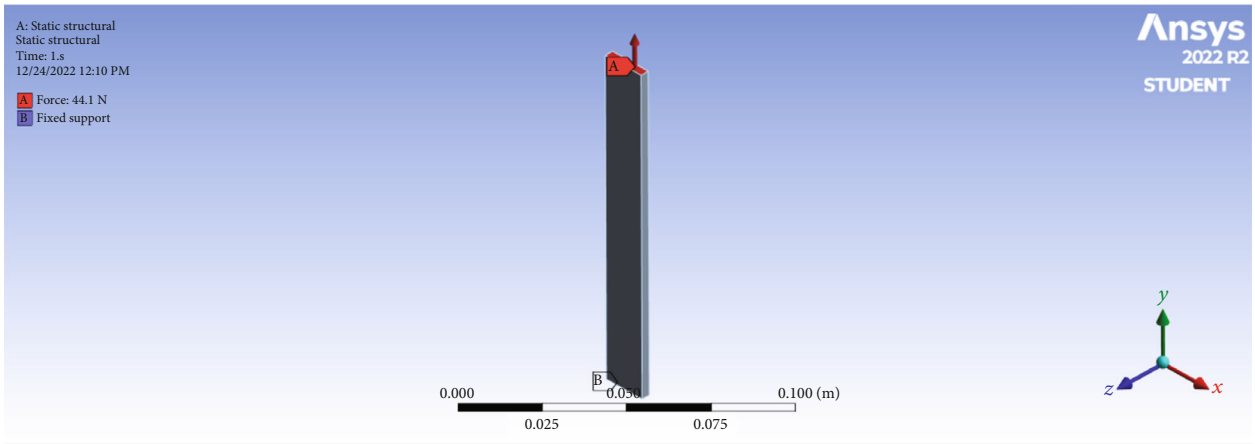

Figure 3: Boundary condition for the model.

Table 3: Material properties of 15 samples.

Run no.	Fibre content (%)	Size of fibre (μm)	Chemical treatments	Tensile strength (MPa)	Yield point (MPa)	Young's modulus (MPa)	Poisson's ratio	Density (g/cm^3)
1	6	150	3	3.599	1.225	10.558	0.369	0.095548
2	2	150	1	4.621	1.943	17.225	0.371	0.059078
3	4	150	2	4.028	3.394	9.518	0.370	0.10665
4	2	75	2	4.362	3.113	10.690	0.368	0.094241
5	6	225	2	2.730	2.710	8.683	0.371	0.117226
6	4	225	1	5.414	2.986	15.648	0.369	0.06466
7	4	225	3	3.573	2.007	8.837	0.372	0.115339
8	4	150	2	4.364	3.725	9.781	0.365	0.101734
9	4	75	1	8.665	4.377	10.931	0.367	0.091912
10	4	75	3	5.717	2.901	15.087	0.371	0.067535
11	2	150	3	3.358	2.767	9.742	0.374	0.105383
12	6	150	1	6.528	5.119	11.574	0.372	0.088136
13	4	150	2	3.942	3.281	9.898	0.367	0.101287
14	6	75	2	5.581	3.764	11.343	0.371	0.089713
15	2	225	2	3.537	2.795	10.446	0.371	0.097355

Table 4: Verification of the model.

Sample no.	Present model		Anirudh et al. [47]		Error (%)
	Fatigue life cycle (min.)	Alternating stress MPa (max.)	Fatigue life cycle (min.)	Alternating stress MPa (max.)	
5	$2.26E^{+05}$	1.0945	$2.26E^{+05}$	1.0945	0
10	$1.00E^{+06}$	0.97565	$1.00E^{+06}$	0.97565	0
15	$3.69E^{+05}$	0.99553	$3.69E^{+05}$	0.99553	0

to Khoathane et al. [35]. Numerous studies have shown that fibre loading has a significant impact on the strength along stiffness of composites made of natural fibre and polymer. Up to a specific degree, the fibre-weight ratio escalates the tensile strength and modulus. In cases where the fibre weight ratio increments beneath the ideal level, the load is dispensed among additional fibres, and because they are well attached to the resin matrix, they have greater tensile qualities [35]. The composites' wear resistance is raised by incrementing the fibre loading. With an increase in fibre loading, these composites' coefficient of friction both rises and falls [36].

Taking into consideration all these various factors for the composite, it is important to understand the various alterations in the mechanical properties of the composite prepared. One such property is the fatigue analysis of the composite. A composite material subjected to repetitive loading degrades over time from discrete microdamage (such as fibre fractures, fibre/matrix debonds, and matrix

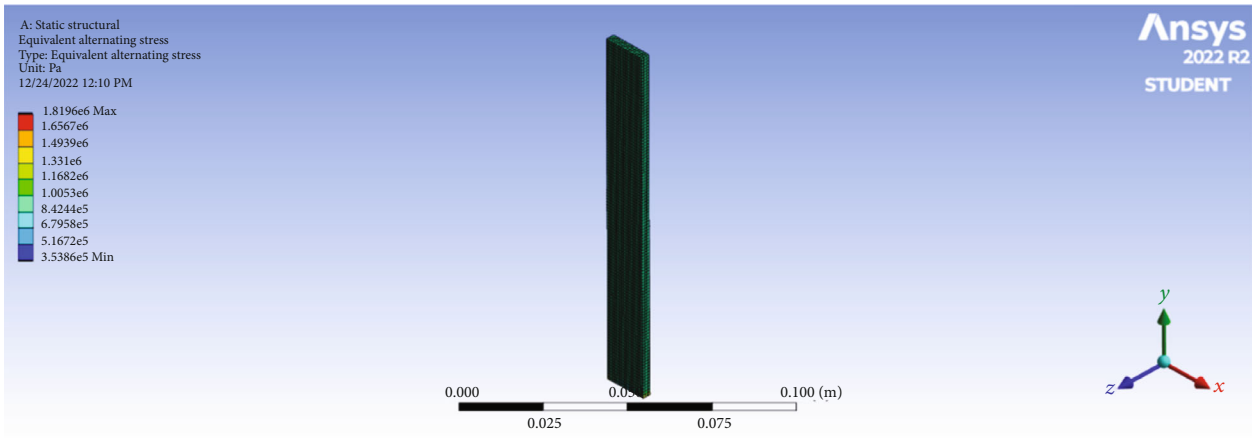

Figure 4: Alternating stress results for a single sample.

Table 5: Fatigue limit from Soderberg's relation.

Sample no.	Fatigue limit (MPa)
1	0.6125
2	0.9715
3	1.697
4	1.5565
5	1.355
6	1.493
7	1.0035
8	1.8625
9	2.1885
10	1.4505
11	1.3835
12	2.5595
13	1.6405
14	1.882
15	1.3975

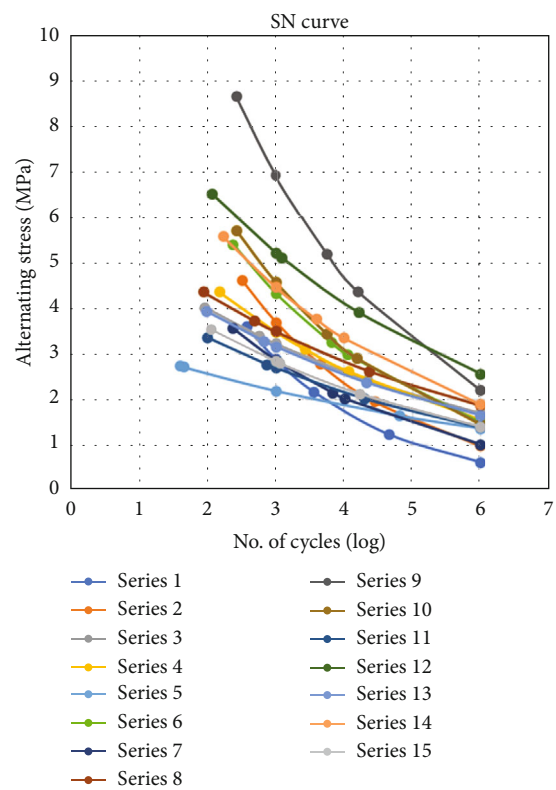

Figure 5: SN curves of 15 samples.

cracking) or macrocrack propagation, sometimes facilitated by a hostile environment like dampness. To guarantee that the product or component is safe for the planned life span or can be replaced before failing, the engineer needs to be aware of how these loading cycles affect the lifetime or component. Fatigue test methods are used to determine a material's resistance to recurrent loading to meet this purpose [37]. These fatigue failures fall under the categories of low-cycle fatigue as well as high-cycle fatigue, which are two domains of cyclic stressing and straining [38]. In comparison to metal, composite material fatigue life prediction is more challenging. This is due to the fact that failure in composite materials does not result from the growth of a single macroscopic crack [39]. The presence of subsidiary constituents as well as the areas where the fibres along with the matrix interact may have a significant effect across the materials' fatigue behaviour. Fatigue qualities for composites can vary significantly because of the vast changes in the characteristics of the fibres and matrix which account for the composite together with the composition of constituents [40]. The work by Gokula Krishnan et al. is based on CNT, fly ash, and coir reinforcement in a polymer composite with an epoxy matrix. It provides analysis showing that the fatigue limit reaches a maximum value of 7.84 MPa in the optimum amalgamation of 1 weight percentage of carbon nanotube, 0.55 weight percentage of coir, and 0.55 weight percentage of fly ash [41].

In accordance with the above literature survey, the following denouements are brought forward.

(i) An examination of many studies and current trends reveals that the demand for materials with qualities

similar to composites reinforced with synthetic fibres but with less negative environmental effects has created a need for composites that are reinforced with natural or plant fibres

(ii) Polypropylene is the most popular matrix/resin used in the creation of coir polymer composites (PP). Epoxy, polylactic acid (PLA), polyster, and polyethylene are listed after that

(iii) However, not enough research has been done on the use of alternative resins such as polyvinyl chloride, polysterene, and vinyl esters in the creation of coir-based composites

(iv) This work attempts to determine the fatigue life analysis of coir-reinforced PVC composites which is a rare one

The authors attempted to develop a numerical procedure to predict the fatigue life of PVC composite which is reinforced with coir fibre. Such attempt is very limited for natural fibre-reinforced composites. The applications of PVC and PVC composites are plenty in day-to-day applications. Hence, its fatigue life prediction is very important. So, the authors develop a numerical procedure to predict the same. The current work is developing a numerical procedure for a natural fibre thermoplastic-reinforced composite.

2. Methodology

The samples are fabricated by considering three parameters: the size of the coir used, the percentage of coir used in fabrication, and the chemical used for the treatment of the coir. The size of the coir is taken between 75 μm and 225 μm. The fibre content is between 2% and 6%, and three types of alkali are considered for the chemical treatment: sodium hydroxide, triethoxy(ethyl)silane, and potassium hydroxide, as mentioned in Table 1. A total of 15 samples are obtained using various parameter combinations, as shown in Table 2. The samples are formed using the RSM (response surface model) tool which comes under DOE (design of experiment), as shown in Figure 1. The RSM uses Box-Behnken designs (BBD) which give a higher-order surface response with an optimum number of samples [42]. The Box-Behnken design is the most effective for an experiment with three components and three levels; also, less testing is required to perform compared to a central composite design [43]. To enumerate the maximum number of experiments (N) essential for the development of the BBD model [44], it is elucidated as follows:

$$N = 2k(k-1) + C_0, \tag{1}$$

where k can be expounded as a number of factors and C_0 can be expounded as the number of central points. As given by the formula, it can be calculated that the total samples are 15 in number.

The 15 sample material properties are referred to by Aravind and Venkatachalam [45]. Various experiments are conducted to enumerate mechanical properties which are used for determining the fatigue limit and SN curve. There is a stress threshold known as a fatigue limit below which a material will not fail from fatigue, regardless of how many load cycles it has experienced [46]. The fatigue limit is imperative for the fatigue analysis which is the ultimate aim of this work and can be computed using the Soderberg relation as referred to in equation (2). As claimed by the ASM handbook, $\sigma_{\max}$ and $\sigma_{\min}$ are taken as 80 per cent and 40 per cent of yield stress, respectively.

Table 6: Results from ANSYS and fatigue life from SN curve.

Samples	Alternating stress (Pa)	Fatigue life
1	$1.81E^{+06}$	8126.995
2	$1.82E^{+06}$	32386.95
3	$1.82E^{+06}$	460956.6
4	$1.81E^{+06}$	239557.6
5	$1.82E^{+06}$	13762.58
6	$1.81E^{+06}$	231398.2
7	$1.82E^{+06}$	18143.04
8	$1.80E^{+06}$	1518763
9	$1.81E^{+06}$	1000000
10	$1.82E^{+06}$	204884.9
11	$1.83E^{+06}$	51314.49
12	$1.82E^{+06}$	1000000
13	$1.81E^{+06}$	335869.1
14	$1.82E^{+06}$	1419613
15	$1.82E^{+06}$	68765.4

$$\frac{\sigma_m}{\sigma_{yt}} + \frac{\sigma_a}{\sigma_e} = 1, \tag{2}$$

where $\sigma_m \longrightarrow$ mean stress $= \sigma_{\max} + \sigma_{\min}/2$, $\sigma_a \longrightarrow$ stress amplitude $= \sigma_{\max} - \sigma_{\min}/2$, $\sigma_e \longrightarrow$ fatigue limit, and $\sigma_{yt} \longrightarrow$ yield stress.

The SN curve is a graph of the alternating stress and the number of cycles before failure and is calculated using the Soderberg equation which is depicted in equation (3). Each material has its own unique SN curve, and it can be calculated through experiments and also using equations. The Soderberg equation is acclimated as its results are based on yield strength in comparison to Goodman's equations which arbitrate ultimate tensile stress. The Soderberg equation is from a linear graph which connects the fatigue limit (σ_e) and yield stress (σ_{yt}). There are 5 values of "S" taken to calculate the SN curve. These are ultimate tensile stress (σ_u), 80% of σ_u, 60% of σ_u, yield stress (σ_{yt}), and 50% of (σ_{yt}). The corresponding no. of cycles is found, and the SN graph is constructed.

$$\text{Log}\, S = (b\text{Log}N) + c, \tag{3}$$

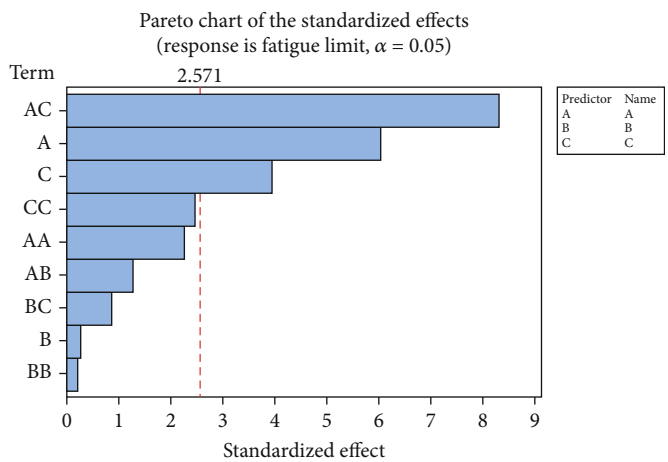

Figure 6: Effect of various parameters on the fatigue limit.

where

$$b = -\frac{1}{3}\log\left[\frac{0.8.\sigma_u}{\sigma_e}\right], \tag{4}$$

$$c = \log\frac{(0.8.\sigma_u)^2}{\sigma_e}. \tag{5}$$

Here, "S" refers to the fatigue stress, "N" is the number of cycles to failure, and "b" and "c" are constants and are derived from equations (4) and (5). σ_u specifies the ultimate tensile stress, and σ_e specifies the fatigue limit.

3. Numerical Analysis

ANSYS software is employed for fatigue simulation. With the aid of ANSYS, it is possible to investigate the strength, elasticity, toughness, temperature distribution, fluid flow, electromagnetism, and other properties of computer-simulated models of structures, electronics, or machine parts. A model of dimensions 115 mm × 15 mm × 3 mm is constructed in SpaceClaim, as shown in Figure 2, and is imported to the ANSYS Workbench for further analysis. The fatigue analysis is performed using the ANSYS Workbench. To do the fatigue analysis, one needs material properties such as yield stress (σ_y), ultimate stress (σ_u), density (ρ), Poisson's ratio (ν), and SN curve, as shown in Figure 3. The yield stress (σ_y), ultimate stress (σ_u), density (ρ), and Poisson's ratio (ν) are obtained from experimental data performed by Aravind and Venkatachalam [45] as given in Table 3. The SN curve is calculated from equations (3) to (5).

Anirudh et al. [47] work is considered to validate our model. The results of the present model are matched with Anirudh et al. [47] with zero error, as given in Table 4.

Hence, the present model is validated. In the model, the geometry is fixed at the bottom plane, and a tensile force of 44.1 N is applied to the top plane. The force is 80% of the force, corresponding to the minimum yield stress.

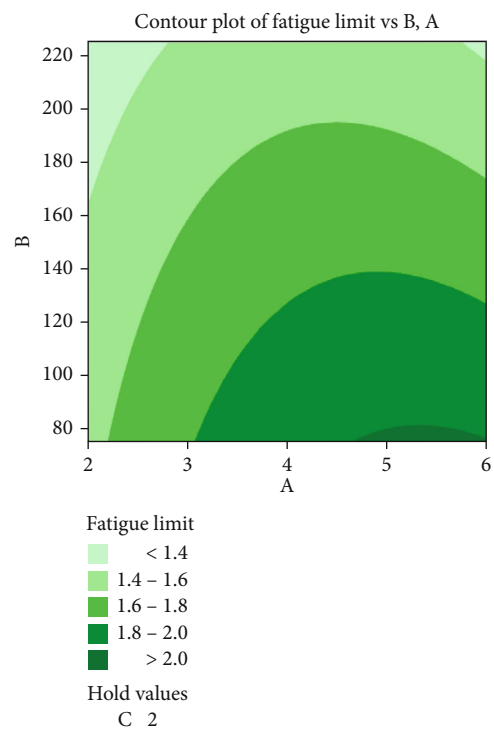

Figure 7: Contour plots of fibre content and fibre size on fatigue limit.

The alternating stress obtained from the fatigue analysis is used to find its corresponding number of cycles from the SN curve; this is deemed to be the fatigue life of that particular sample, as shown in Figure 4.

4. Results and Discussion

In this work, Soderberg's equation is chosen to fix the fatigue loading conditions for the analysis to obtain fatigue values in the fatigue solver of ANSYS. The fatigue limit is calculated from the Soderberg relation (equation (2)), and the results are tabulated in Table 5.

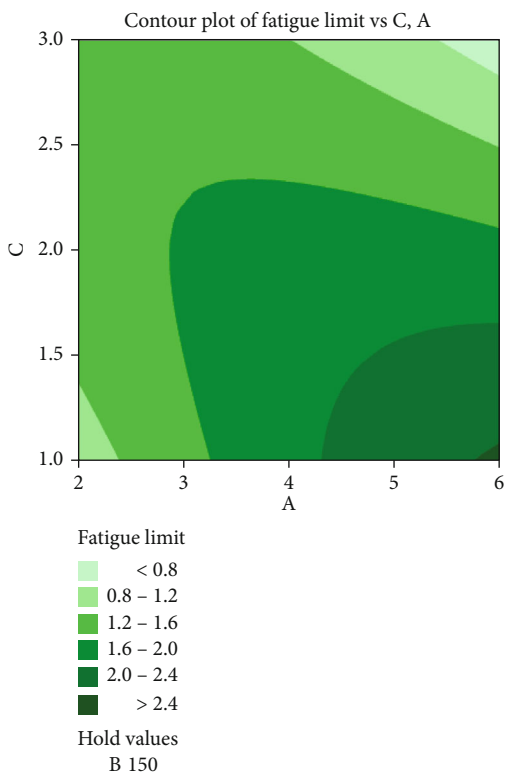

Figure 8: Contour plots of fibre content and chemical on fatigue limit.

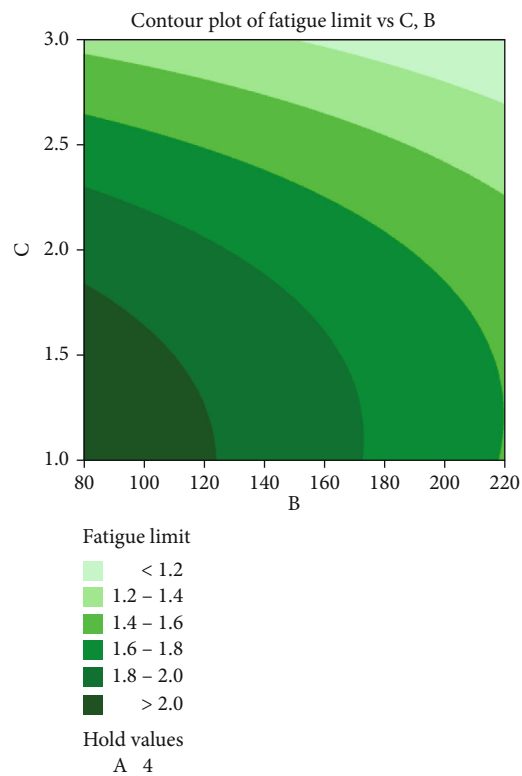

Figure 9: Contour plots of chemical and fibre size on the fatigue limit.

The simulation uses an alternating load at one end of the strip in the in-plane tensile direction with a magnitude of 44.1 N based on the minimum yield strength of the test samples. The fixed support in all six degrees of freedom is located at the opposite end of the strip. The maximal induced alternate stress, determined by the minimum number of cycles to fail and Von Mises stress, is computed and utilized in the analysis of variance. The SN curves of the 15 samples are calculated from Soderberg's equation (2). Figure 5 shows the SN curves of 15 samples put together. This graph has an important role in analyzing the material fatigue life of the samples.

The results obtained from the fatigue analysis carried out using the ANSYS Workbench are tabulated in Table 5. The fatigue life of the materials is interpreted from the SN curve graph, taking the alternating stress found from ANSYS. Also, Table 6 represents the fatigue life from the SN curve.

4.1. ANOVA Analysis. The statistical method known as analysis of variance (ANOVA) is used to examine how different means differ from one another. Minitab is the software used for this analysis. The Minitab gives the regression equation consolidated from the three parameters and the fatigue limit of the samples. The equation gives statistical values for a better understanding of the influence of the 3 parameters on the fatigue limit.

The Pareto chart depicts the effects of various parameters. In Figure 6, the Pareto chart shows that the fibre size and the chemicals used for treatment have the major influence when considering the fatigue limit, and fibre size has the least influence. Figures 7–9 depict the comparisons between the parameters taking a combination of the parameters in pairs. The inferences obtained from the graph are listed one by one. The fibre content maximizes the fatigue limit when the fibre content percentage is at its maximum. Contrastingly, the size of the fibre is required to be in lower ranges to get the optimum fatigue limit. Among the three chemicals, triethoxy(ethyl)silane is the best chemical for providing an effective increment in the fatigue limit.

The main effect plot (Figure 10) helps us understand individual parameters' effects on the fatigue limit. Figure 10(a) shows that a rise in fibre content from 2 wt.% to 4 wt.% increases fatigue life, but a decrease is also observed from 4 wt.% to 6 wt.% of fibre content. Figure 10(b) shows that fatigue life decreases when particle size is increased from 75 μm to 225 μm. Figure 10(c) reveals that fatigue life is high for triethoxy(ethyl)silane chemically treated FRP (fibre-reinforced polymer) composites. The hydroxyl groups (lignin, hemicellulose, and pectin) existing in the coir powder are reduced, thereby increasing the cellulose content. As a result, a good interfacial bond is created, which leads to an increase in fatigue life. Larger amounts of lignin, hemicellulose, and pectin are removed by triethoxy(ethyl)silane compared to other chemical treatments. Hence, the silane treatment leads to a higher fatigue life in comparison to other treatments. Figure 10 concludes that there is an increase in fatigue limit as the fibre content increases from 2% to 4%, and the decrease in fatigue limit is gradual with an increase in the size of fibre. Triethoxy(ethyl)silane is concluded to be the most influential among the chemicals used for the treatment of the fibre.

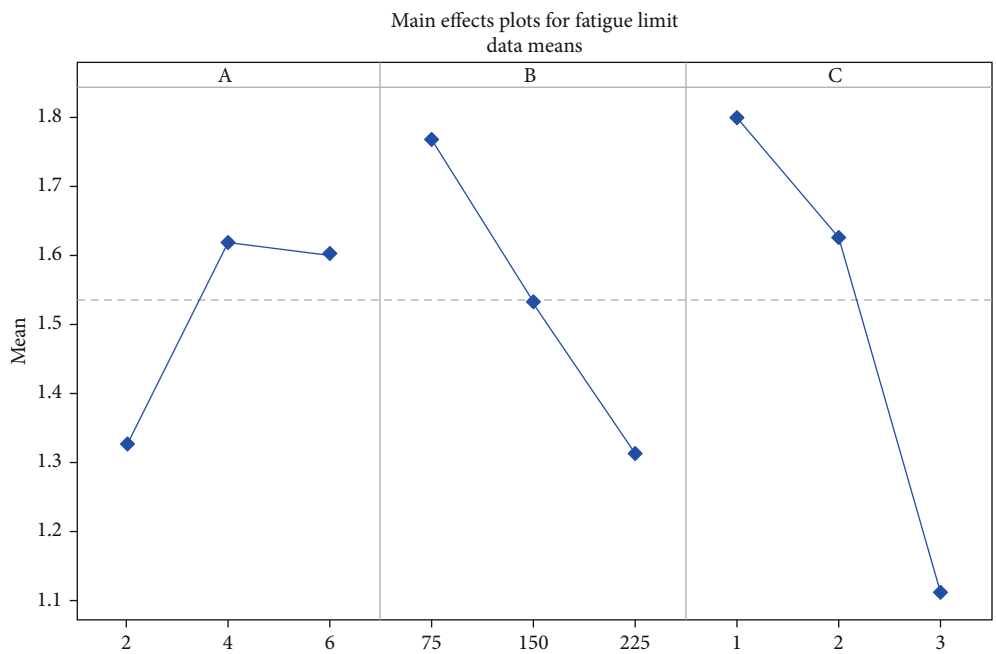

Figure 10: Main effect plots for fatigue limit with three parameters.

Table 7: Error analysis of the values procured from Soderberg's relation and regression equation.

Fibre content (wt.%)	Fibre size (μm)	Chemical treatment	Fatigue limit (MPa) from Soderberg's relation	Fatigue limit (MPa) from the regression equation	Error (%)
6	150	3	0.6125	0.5827	4.865306
2	150	1	0.9715	0.9985	-2.77921
4	150	2	1.697	1.7319	-2.05657
2	75	2	1.5565	1.546175	0.663347
6	225	2	1.355	1.362375	-0.54428
4	225	1	1.493	1.586225	-6.24414
4	225	3	1.0035	1.020025	-1.64674
4	150	2	1.8625	1.7319	7.012081
4	75	1	2.1885	2.168825	0.899018
4	75	3	1.4505	1.354225	6.637366
2	150	3	1.3835	1.4877	-7.53162
6	150	1	2.5595	2.4527	4.17269
4	150	2	1.6405	1.7319	-5.57147
6	75	2	1.882	2.004675	-6.51833
2	225	2	1.3975	1.271675	9.003578

Regression (equation (6)) is a second-order polynomial equation obtained through Minitab based on the parameters A, B, and C is as follows:

$$\begin{aligned}\text{Fatigue limit} = &-1.346 + 1.088A - 0.00136B + 1.441C \\ &- 0.0422A * A - 0.000003B * B - 0.1827C \\ &* C - 0.000613A * B - 0.2949A \\ &* C + 0.000828B * C,\end{aligned} \tag{6}$$

where "A" is the fibre content, "B" is the fibre size, and "C" is the chemical used for treatment. The fatigue limits obtained from the regression equation and the fatigue limits obtained from the Soderberg equation are compared, and the error percentage is below 10%, as given in Table 7. This gives credit to the efficiency of the regression equation.

4.2. Verification and Optimization of the Model. The response optimization plot is used to find the optimal combinations to create a significant fatigue limit. In Figure 11, a response optimization plot for fatigue limit is shown, with

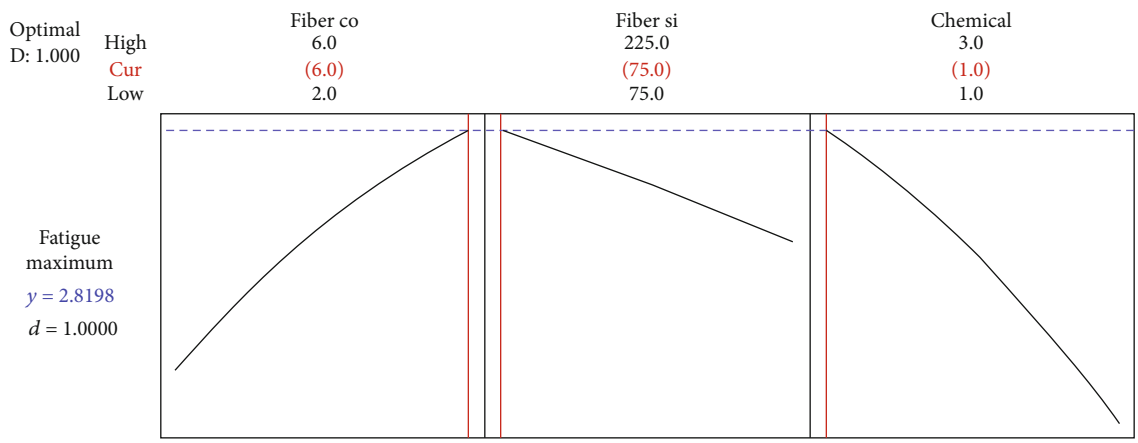

Figure 11: Response optimization plot for fatigue limit.

Table 8: Criterion for optimization.

Solution	Fibre content (%)	Fibre size (μm)	Chemical treatments	Fatigue limit fit	Composite desirability
1	6	75	1	2.819	1

Table 9: Optimum set of parameters.

S. no.	Fibre content (%)	Fibre size (μm)	Chemical treatments	Fatigue limit (MPa) from Soderberg's relation	Optimization	Error (%)
1	6	75	1	2.947	2.819	4.54

the Y-axis displaying fatigue limit and the X-axis exhibiting fibre content (%), fibre size (μm), and chemical treatments. It exhibits that a combination of fibre content (6%), fibre size (75 μm), and triethoxy(ethyl)silane treatment offers a high fatigue limit (2.819 MPa).

To attain a high fatigue limit, it is essential to recognize the maximum significance of each parameter by satisfying composite desirability. Thus, the optimized combination provides a maximum fatigue limit, as stated in Table 8.

Table 9 explicates the validation test for the optimization process and displays the error examination for the fatigue limit among Soderberg's relation and optimization values. The error is 4.54% which shows the legitimacy of the optimization process.

5. Conclusion

The coir-reinforced PVC composite, with varying fibre content, fibre size, and the different chemicals treated, is simulated using ANSYS for fatigue analysis. Various statistical analyses are performed to predict the optimized fatigue limit. The analysis has led the way to the following inferences and results:

(i) The fibre content which is the weight percentage of coir present in the composite should be 5%-6% of the weight for acquiring a composite with a maximum fatigue limit

(ii) The fatigue limit is augmented when the size of the coir is 75-120 μm, where the results are improved in lower ranges

(iii) The chemical treatment of coir is necessary for improving the adhesion of the fibre in composite use. The coir chemically treated with triethoxy(ethyl)silane shows an ameliorated value of the fatigue limit

(iv) Using a response optimizer, a high fatigue limit (2.819 MPa) is obtained for a combination of fibre content (6%), fibre size (75 μm), and triethoxy(ethyl)silane treatment

Data Availability

The data for the present investigation are available and can be submitted whenever required.

Conflicts of Interest

The authors declare that they have no conflicts of interest.

References

[1] R. Wirawan, E. S. Zainudin, and S. M. Sapuan, "Mechanical properties of natural fibre reinforced PVC composites: a review," *Sains Malaysiana*, vol. 38, no. 4, pp. 531–535, 2009.

[2] D. Willoughby, *Plastic Piping Handbook*, McGraw-Hill, New York, 2002.

[3] W. I. J. Zaini, M. Y. A. Fuad, Z. Ismail, M. S. Mansor, and J. Mustafah, "The effect of filler content and size on the mechanical properties of polypropylene/oil palm wood flour composites," *Polymer International*, vol. 40, no. 1, pp. 51–55, 1996.

[4] M. Y. Khalid, A. Al Rashid, Z. U. Arif, W. Ahmed, H. Arshad, and A. A. Zaidi, "Natural fiber reinforced composites: sustainable materials for emerging applications," *Results in Engineering*, vol. 11, article 100263, 2021.

[5] H. Ku, H. Wang, N. Pattarachaiyakoop, and M. Trada, "A review on the tensile properties of natural fibre reinforced polymer composites," *International Journal of Composites Part B: Engineering*, vol. 42, no. 4, pp. 856–873, 2011.

[6] S. N. Monteiro, L. A. H. Terrones, and J. R. M. D'Almeida, "Mechanical performance of coir fiber/polyester composites," *Polymer Testing*, vol. 27, no. 5, pp. 591–595, 2008.

[7] N. Ayrilmis, S. Jarusombuti, V. Fueangvivat, P. Bauchongkol, and R. H. White, "Coir fiber reinforced polypropylene composite panel for automotive interior applications," *Fibers and Polymers*, vol. 12, no. 7, pp. 919–926, 2011.

[8] S. Harish, D. Peter Michael, A. Bensely, D. Mohan Lal, and A. Rajadurai, "Mechanical property evaluation of natural fiber coir composite," *Materials Characterization*, vol. 60, no. 1, pp. 44–49, 2009.

[9] S. Shinoj, R. Visvanathan, S. Panigrahi, and M. Kochubabu, "Oil palm fiber (OPF) and its composites: a review," *Industrial Crops and Products*, vol. 33, no. 1, pp. 7–22, 2011.

[10] A. V. Ratna Prasad and K. Mohana Rao, "Mechanical properties of natural fibre reinforced polyester composites: jowar, sisal and bamboo," *Materials & Design*, vol. 32, no. 8-9, pp. 4658–4663, 2011.

[11] K. Joseph, R. D. Tolêdo Filho, B. James, S. Thomas, and L. H. D. Carvalho, "A review on sisal fibre reinforced polymer composites," *Revista Brasileira de Engenharia Agrícola e Ambiental*, vol. 3, no. 3, pp. 367–379, 1999.

[12] S. Jain, R. Kumar, and U. C. Jindal, "Mechanical behaviour of bamboo and bamboo composite," *Journal of Materials Science*, vol. 27, no. 17, pp. 4598–4604, 1992.

[13] S. M. Sapuan, A. Leenie, M. Harimi, and Y. K. Beng, "Mechanical properties of woven banana fibre reinforced epoxy composites," *Materials & Design*, vol. 27, no. 8, pp. 689–693, 2006.

[14] N. Amir, K. A. Z. Abidin, and F. B. M. Shiri, "Effects of fibre configuration on mechanical properties of banana fibre/PP/MAPP natural fibre reinforced polymer composite," *Procedia Engineering*, vol. 184, pp. 573–580, 2017.

[15] J. António, A. Tadeu, B. Marques, J. A. S. Almeida, and V. Pinto, "Application of rice husk in the development of new composite boards," *Construction and Building Materials*, vol. 176, pp. 432–439, 2018.

[16] S. Fatima and A. R. Mohanty, "Acoustical and fire-retardant properties of jute composite materials," *Applied Acoustics*, vol. 72, no. 2-3, pp. 108–114, 2011.

[17] H. Wang, H. Memon, E. A. M. Hassan, M. S. Miah, and M. A. Ali, "Effect of jute fiber modification on mechanical properties of jute fiber composite," *Materials*, vol. 12, no. 8, p. 1226, 2019.

[18] N. Saba, M. T. Paridah, and M. Jawaid, "Mechanical properties of kenaf fibre reinforced polymer composite: a review," *Construction and Building Materials*, vol. 76, pp. 87–96, 2015.

[19] H. M. Akil, M. F. Omar, A. A. M. Mazuki, S. Safiee, Z. A. M. Ishak, and A. Abu Bakar, "Kenaf fiber reinforced composites: a review," *Materials & Design*, vol. 32, no. 8-9, pp. 4107–4121, 2011.

[20] T. Raja and A. Palanivel, "Evaluation of mechanical properties of natural fibre reinforced composites - a review," *International Journal of Mechanical Engineering and Technology*, vol. 8, no. 7, pp. 915–924, 2017.

[21] N. Jauhari, R. Mishra, and H. Thakur, "Natural fibre reinforced composite laminates – a review," *Materials Today: Proceedings*, vol. 2, no. 4-5, pp. 2868–2877, 2015.

[22] M. Sood and G. Dwivedi, "Effect of fiber treatment on flexural properties of natural fiber reinforced composites: a review," *Egyptian Journal of Petroleum*, vol. 27, no. 4, pp. 775–783, 2018.

[23] X. Li, L. G. Tabil, and S. Panigrahi, "Chemical treatments of natural fiber for use in natural fiber-reinforced composites: a review," *Journal of Polymers and the Environment*, vol. 15, no. 1, pp. 25–33, 2007.

[24] M. M. Kabir, H. Wang, K. T. Lau, and F. Cardona, "Chemical treatments on plant-based natural fibre reinforced polymer composites: an overview," *Composites Part B: Engineering*, vol. 43, pp. 2883–2892, 2012.

[25] M. Aravindh, S. Sathish, R. Ranga Raj et al., "A review on the effect of various chemical treatments on the mechanical properties of renewable fibre-reinforced composites," *Advances in Materials Science and Engineering*, vol. 2022, Article ID 2009691, 24 pages, 2022.

[26] G. Venkatachalam, N. Mehta, S. Shukla et al., "Experimental investigations on flexural and fracture behaviors of flax fibre reinforced sandwich panels," *International Review of Mechanical Engineering*, vol. 12, pp. 231–238, 2018.

[27] A. G. Adeniyi, D. V. Onifade, J. O. Ighalo, and A. S. Adeoye, "A review of coir fibre reinforced polymer composites," *Composites: Part A*, vol. 41, pp. 192–198, 2010.

[28] M. Ishizaki, L. Visconte, C. Furtado, M. Leite, and J. Leblanc, "Mechanical and morphological characterization of polypropylene and green coconut fibre composites: influence of fibre content and mixture conditions," *Polímeros*, vol. 16, pp. 182–186, 2005.

[29] V. G. Geethamma, R. Joseph, and S. Thomas, "Short coir fibre-reinforced natural rubber composites: effects of fibre length, orientation, and alkali treatment," *Journal of Applied Polymer Science*, vol. 36, no. 11, pp. 1495–1506, 2005.

[30] S. K. Saw, G. Sarkhel, and A. Choudhury, "Preparation and characterization of chemically modified jute-coir hybrid fiber reinforced epoxy novolac composites," *Journal of Applied Polymer Science*, vol. 125, no. 4, pp. 3038–3049, 2012.

[31] A. G. Adeniyi, D. V. Onifade, J. O. Ighalo, and A. S. Adeoye, "A review of coir fiber reinforced polymer composites," *Composites Part B: Engineering*, vol. 176, article 107305, 2019.

[32] V. Gopalan, V. Pragasam, A. Ingle, A. A. Kazi, G. Mannayee, and R. Dam, "The effect of fibre size on tensile characteristics of natural-fibre-reinforced composites," *Emerging Materials Research*, vol. 8, no. 3, pp. 426–433, 2019.

[33] N. S. Sadeq, Z. G. Mohammadsalih, and R. H. Mohammed, "Effect of grain size on the structure and properties of coir epoxy composites," *SN Applied Sciences*, vol. 2, no. 7, p. 1191, 2020.

[34] A. S. Singha and R. K. Rana, "Natural fibre reinforced polystyrene composites: effect of fibre loading, fibre dimensions and surface modification on mechanical properties," *Materials & Design*, vol. 41, pp. 289–297, 2012.

[35] M. C. Khoathane, O. C. Vorster, and E. R. Sadiku, "Hemp fiber-reinforced 1-pentene/polypropylene copolymer: the

effect of fiber loading on the mechanical and thermal characteristics of the composites," *Journal of Reinforced Plastics and Composites*, vol. 27, no. 14, pp. 1533–1544, 2008.

[36] L. Kerni, S. Singh, A. Patnaik, and N. Kumar, "A review on natural fiber reinforced composites," *Materials Today: Proceedings*, vol. 28, pp. 1616–1621, 2020.

[37] B. Harris, *Fatigue in Composites: Science and Technology of the Fatigue Response of Fibre-Reinforced Plastics*, Woodhead Publishing, 2003.

[38] F. Wu and W. Yao, "A fatigue damage model of composite materials," *International Journal of Fatigue*, vol. 32, no. 1, 2009.

[39] M. J. Suriani, A. Ali, S. M. Sapuan, and A. Khalina, "Aspect of fatigue analysis of composite materials: a review," *Journal of Science & Technology - Pertanika*, vol. 21, no. 1, pp. 1–14, 2013.

[40] H. Mao and S. Mahadevan, "Fatigue damage modelling of composite materials," *Composite Structures*, vol. 58, no. 4, pp. 405–410, 2002.

[41] B. Gokula Krishnan, G. Venkatachalam, and A. Deshmukh, "Prediction of fatigue life of full penetration weld joint using thermal elasto plastic properties incorporating residual stress effect," *UPB Scientific Bulletin, Series D*, vol. 83, no. 1, 2021.

[42] V. Gopalan, P. Bhardwaj, N. Satonkar, and V. Pragasam, "determination of fatigue limit of coir/CNT/fly ash reinforced epoxy polymer matrix composite," *Periodica Polytechnica Mechanical Engineering*, vol. 64, no. 3, pp. 248–255, 2020.

[43] J. S. Rao and B. Kumar, "3D blade root shape optimization," in *10th International Conference on Vibrations in Rotating Machinery*Woodhead Publishing.

[44] M. Manohar, J. Joseph, T. Selvaraj, and D. Sivakumar, "Application of Box Behnken design to optimize the parameters for turning Inconel 718 using coated carbide tools," *International Journal of Scientific & Engineering Research*, vol. 4, no. 4, 2013.

[45] S. Aravindh and G. Venkatachalam, "Investigation on elastic constants of microfibril reinforced poly vinyl chloride composites using impulsive excitation of vibration," *Polymers*, vol. 14, no. 23, p. 5083, 2022.

[46] F. C. Campbell, "Fatigue," in *Elements of Metallurgy and Engineering Alloys*, F. C. Campbell, Ed., pp. 243–264, ASM International, 2008.

[47] V. P. Anirudh, S. A. Ajay Krishna, A. Akshat, G. Venkatachalam, and T. G. Loganathan, "Virtual fatigue analysis of epoxy based composite reinforced with sugarcane fibre, fly ash and carbon nano tubes," *Materialwissenschaft und Werkstofftechnik*, vol. 53, no. 1, pp. 56–67, 2022.